frontiers in Materials

ORIGINAL RESEARCH
published: 20 December 2021
doi: 10.3389/fmats.2021.802468

Vanadium and Tannic Acid-Based Composite Conversion Coating for 6063 Aluminum Alloy

*Wen Zhu, Furui Chen, Youbin Luo, Zhijun Su, Wenfang Li *, Aihua Yi, Zhongmiao Liao, Kang Li, Ken Chen, Yiwen Hu, Yashu Xu and Sinan Guo*

School of Material Science and Engineering, Dongguan University of Technology, Dongguan, China

In this study, a vanadium (V) and tannic acid-based composite conversion coating (VTACC) was prepared on 6063 aluminum alloy (AA6063) to increase its corrosion resistance. The surface morphology and compositions of the VTACCs were characterized using scanning electron microscopy (SEM), energy dispersive spectrometry (EDS), and X-ray photoelectron spectroscopy (XPS). The corrosion resistance of the coatings was investigated by linear polarization and electrochemical impedance spectra (EIS). The self-healing ability of the coating was detected by SEM, EDS, and scanning vibrating electrode technique (SVET) measurements. The coating mainly consisted of metal oxides, including Al_2O_3, VO_2, V_2O_3, and V_2O_5, and metal organic complexes (Al and V-complexes). The electrochemical measurement results indicated that the best corrosion resistance of VTACC was acquired when the treatment time was 12 min. Furthermore, because a new coating with vanadium rich oxide was developed on the scratch area, artificial scratch VTACC surfaces were repaired after several days of immersion in 3.5-wt% NaCl solution.

Keywords: aluminum alloy, conversion coating, self-healing, SVET, corrosion resistance

OPEN ACCESS

Edited by:
Hao Zhang,
Jiangxi Science and Technology Normal University, China

Reviewed by:
Rongfa Zhang,
Jiangxi Science and Technology Normal University, China
Jiantao Qi,
China University of Petroleum (Huadong), China

****Correspondence:***
Wenfang Li
mewfli@163.com

Specialty section:
This article was submitted to Polymeric and Composite Materials, a section of the journal Frontiers in Materials

Received: *26 October 2021*
Accepted: *22 November 2021*
Published: *20 December 2021*

Citation:
Zhu W, Chen F, Luo Y, Su Z, Li W, Yi A, Liao Z, Li K, Chen K, Hu Y, Xu Y and Guo S (2021) Vanadium and Tannic Acid-Based Composite Conversion Coating for 6063 Aluminum Alloy. Front. Mater. 8:802468. doi: 10.3389/fmats.2021.802468

1 INTRODUCTION

Aluminum (Al) alloys have numerous industrial applications because of their high mechanical performance and low density (Dursun and Soutis, 2014). However, they are readily affected by various types of corrosion, such as intergranular corrosion, stress corrosion cracking, exfoliation, and pitting corrosion (Gerengi et al., 2015). Therefore, surface modification treatments, for example, electroplating (Chen et al., 2011), anodization (Bertram et al., 2014), micro-arc oxidation (Li et al., 2020), and chemical conversion (Twite and Bierwagen, 1998), have been developed to improve the corrosion resistance of Al alloys. Among these methods, the conversion treatment technique is known for its low-cost and operation simplicity. Chromate conversion coatings are one of the most widely used on Al alloys for their excellent corrosion resistance, particular self-healing, and good organic coating adhesion (Campestrini et al., 2004a; Campestrini et al., 2004b; Campestrini et al., 2016). Nevertheless, its utilization has been banned by relevant environmental directives due to hexavalent chromium [Cr (VI)] in the conversion solution and the coating has a wide toxicity to human health and ecological environment (Lay and Levina, 1998; Zhitkovich et al., 2000; Quievryn et al., 2003; Nordberg et al., 2007). As a consequence, various non-chromate conversion coatings have been exploited in the last few decades, including phosphate (Shida et al., 2003; Sheng et al., 2010), molybdate (Huang et al., 2019; Chen and Xu, 2021), rare-earth metal salts (Aziz et al., 2011; Zuo et al., 2014), vanadate (Vega et al., 2011; Niu et al., 2014), and zirconate and/or titanate (Lunder et al., 2004; Guan et al., 2011; Yi et al., 2012; Zuo et al., 2015).

TABLE1 | Main chemical elements and compositions of the 6063 Al alloy (wt.%).

Elements	Si	Mg	Fe	Mn	Cu	Cr	Zn	Ti	Al
Content	0.51	0.85	0.33	0.07	0.15	0.20	0.17	0.08	Bal.

Among the above chromate-free conversion methods, vanadium (V)-based conversion treatment has become a research focus as a feasible replacement for chromate conversion coatings because of its self-healing performance. V, similar to chromium (Cr), is a polyvalent state metal and can form a variety of soluble and insoluble oxides, which can form a cathodic inhibitor and posses a self-healing property by releasing dissolved oxide. Yang et al. (2015) have reported the preparation of V-based conversion coating on AZ61 magnesium (Mg) alloy and its improvement for the corrosion resistance of this alloy. The results showed that the best technological parameters of the coatings were 80°C for 10 min in 30 g/L $NaVO_3$ solution. Hamdy et al. (2011) have investigated the self-healing performance of V-based conversion coatings on ZE41 Mg alloy substrates. Their results showed that the soluble oxidation state in the vanadate conversion coating played a key role in self-healing process, which is the same as the soluble Cr(VI) oxides in chromate conversion coatings. Kun et al. (Li et al., 2015) have investigated the effects of vanadia solution concentration, pH, and treating temperature on the corrosion resistance of vanadia coatings on AZ31 Mg alloy. Their results showed that the best operating conditions were 0.6 M $NaVO_3$ conversion solution and pH 4 at 60°C and the best coating showed excellent self-healing performance. Tannic acid is an environmentally friendly organic compound which can react with metal ions to form metal-organic complexes to improve the corrosion resistance of the coatings (Zhang et al., 2012; Cui et al., 2018). In our previous work, tannic acid was used as an addition to Ti/Zr/V conversion solution, which improved effectively the corrosion resistance of the AA6063 by forming an insoluble metal-tannate complex (Zhu et al., 2016; Zhu et al., 2017).

Most studies have focused on a single V solution and there have been few appropriate studies regarding the effects of organic additions on V-based conversion coatings. In this study, a vanadate and tannic acid composite conversion coating (VTACC) was prepared on AA6063 as a new alternative for chromate conversion coating. Surface characterization of the VTACC was performed using scanning electron microscopy (SEM), scanning electron microscopy (SEM), and X-ray photoelectron spectroscopy (XPS). The corrosion resistance and self-healing ability of the coating was evaluated by SEM, EDS, and scanning vibrating electrode technique (SVET).

2 EXPERIMENTAL PROCEDURE

2.1 Substrate and Conversion Coating Preparation

The main chemical elements and compositions of AA6063 are presented in **Table 1**. Samples were prepared to two different specifications, 30 × 30 × 2 mm and 20 × 20 × 2 mm, and then polished with SiC sandpaper up to 1,200 grit. Prior to the conversion treatment, samples were immersed in industrial acid at room temperature for 1 min, washed with distilled water, and then cleaned in mixed acid at room temperature for 2 min to activate substrate surfaces and then rinsed with distilled water. The chemical compositions of industrial acid and mixed acid were reported in previous work shown in Ref (Zhu et al., 2017). Finally, activated samples were immersed in VTA-based conversion solution, which was composed of 2 g/L $NaVO_3$ and 2 g/L tannin acid, and hydrofluoric acid solution was used to adjust the pH value to 2.8.

2.2 Testing

2.2.1 Surface Analysis

The surface morphology and compositions of the VTACCs on AA6063 were investigated using a field emission Nova-Nano SEM-230 scanning electron microscope (FE-SEM) with an EDS (FEI Co., Hillsboro, OR, United States) and an X-ray photoelectron spectroscope (XPS; Thermo Fisher Scientific Inc., Waltham, MA, United States) equipped with a standard Al-Kα X-ray source and a hemisphere electron energy analyzer in an extreme vacuum chamber, with a 10^{-9} bar base pressure to detect the layer composition. All spectral binding energies were corrected per the reference standard binding energy of the C-1s peak at 284.6 eV. The chemical reaction of V and TA was characterized by FT-IR using a Vertex70 Bruker spectrophotometer with an attenuated total reflectance accessory (Bruker Corp., Billerica, MA, United States; energy scanning from 590 to 4,000 cm^{-1} and resolution at 4 cm^{-1}).

2.2.2 Electrochemical Measurement

The corrosion resistance of the VTACC was examined using an EIS experiment on the CHI660E electrochemical work station (CH Instruments, Inc., Austin, TX, United States) in 3.5-wt.% NaCl solution. The typical three-electrode system was composed of the VTACC sample with an exposed area of 1 cm^2 a saturated calomel electrode (SCE), and a platinum foil as the working, the reference, and the counter electrodes, respectively. The EIS test was performed after the sample obtained a stable open-circuit potential, with an amplitude of 5 mV, test frequency range of 0.01 Hz–100 kHz, and sample exposure area at a constant 1 cm^2. The Tafel plot data was acquired at a scan rate of within a scan range between −0.2 and −1.2 V using 1 mV/s.

2.2.3 Scanning Vibrating Electrode Technique

The SVET measurements were carried out with a scanning electrochemical microscope system (Princetion Applied VersaSCAN, Ametek, Inc., Berwyn, PA, United States) to evaluate the self-healing tendency of VTACC after immersion in 3.5-wt.% NaCl solution for different times. The working, reference, and counter electrode were a platinum-disk microelectrode of 10 μm diameter, Ag/AgCl, KCl (sat) electrode, and a platinum plate, respectively.

Prior to each examination, AA6063 samples were embedded in epoxy resin using mixture of 25 ml (epoxy resin) and 15 ml (epoxy hardener) at room temperature for 24 h, polished with SiC sandpaper up to 1,200 grit, and then immersed in VTA solution

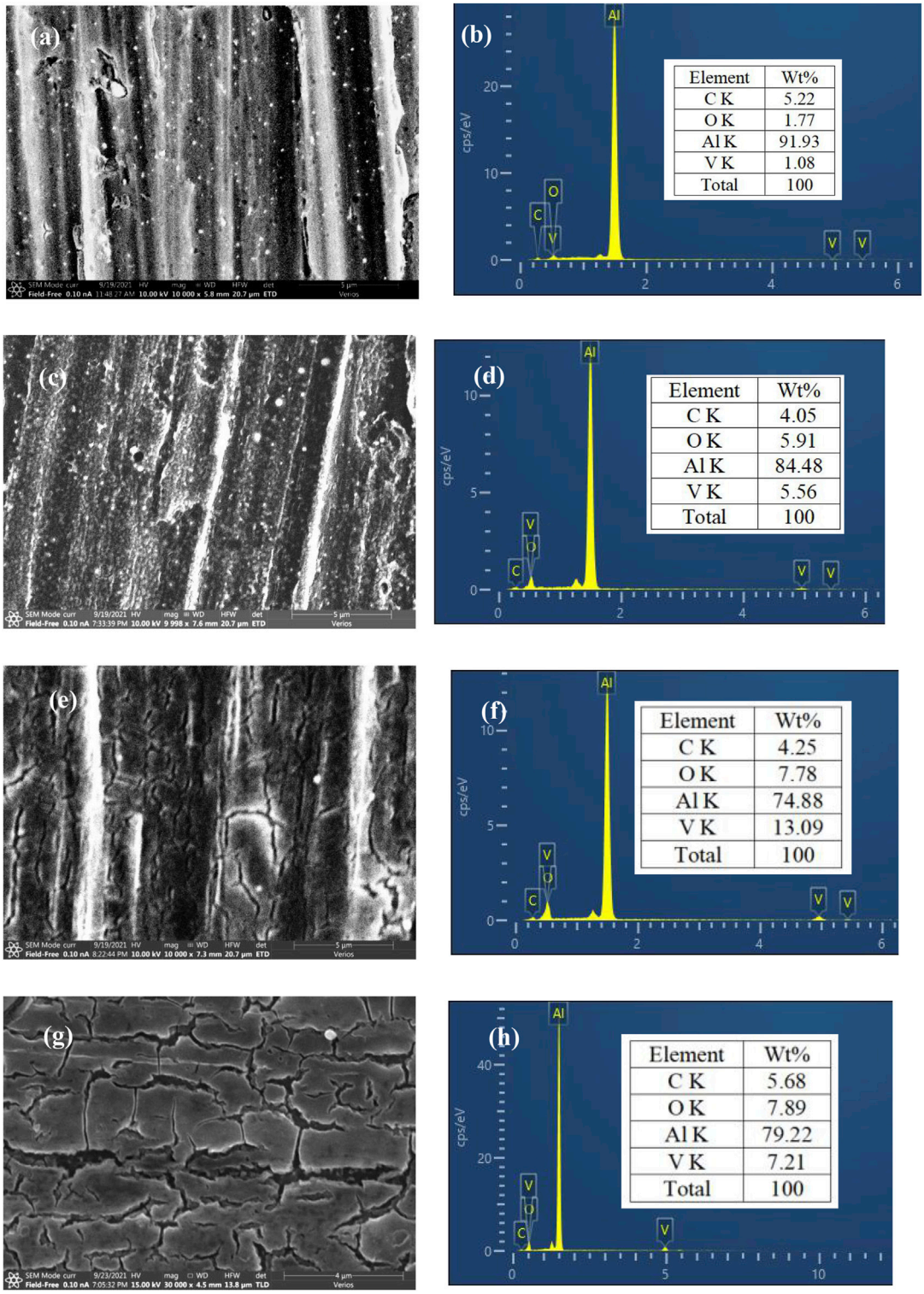

FIGURE 1 | SEM images and EDS results of AA 6063 samples treated in the VTA conversion solution for different treatment times: 5 min **(A,B)**, 10 min **(C,D)**, 15 min **(E,F)**, and 20 min **(G,H)**.

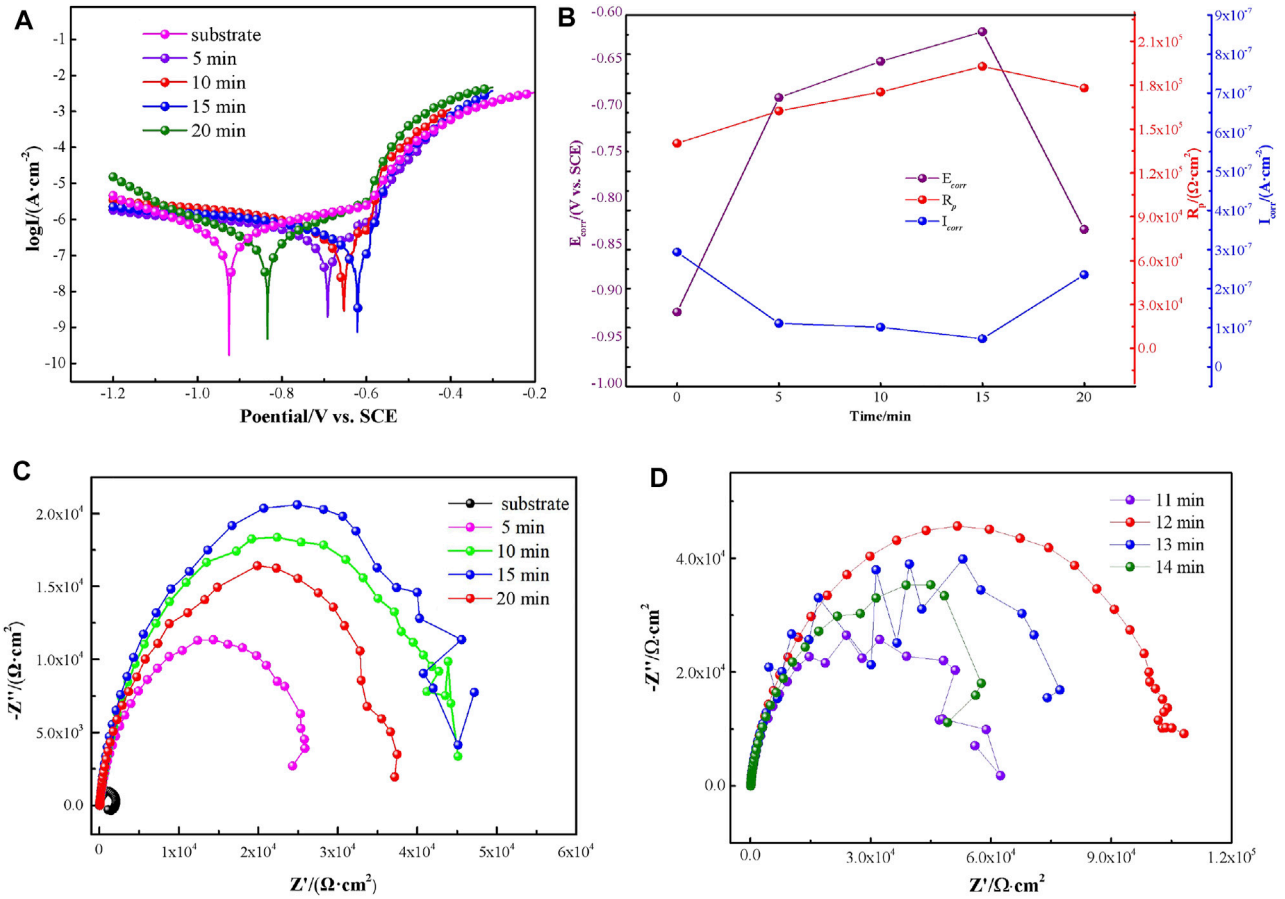

FIGURE 2 | Polarization curves **(A)**, corresponding corrosion dates **(B)**, and Nyquist plots **(C,D)** of VTACCs obtained from different treatment times.

for conversion treatment. The tip-sample distance was controlled at 20 μm. Scans were performed within the scope of 1,000 × 1,000 μm^2 area with a relative scan rate of 50 μm s^{-1}.

3 RESULTS AND DISCUSSION

3.1 SEM Analysis

SEM images and EDS results of AA6063 samples after immersion in VTA-based solution for 5, 10, 15, and 20 min exhibited that mechanical scratches, granules, and long grooves were observed on samples surfaces, which was mainly produced by brittle particles fracturing and/or debris embedded in the substrate as it was processed (**Figure 1A**) (Koroleva et al., 1999). VTACC had just started and not enough to cover the substrate surface after 5 min of conversion solution immersion and the V signal was exceedingly weak from EDS analysis results (**Figure 1B**). When the treatment time increased to 10 min, scallops on the sample's surface became shallow due to the formation of a thicker VTACC coating on the alloy (**Figures 2C,D**). With an increased treatment time of 15 min, a compact and smooth coating was produced that nearly covered the substrate and the V content as high as 13.09 wt % (**Figures 1E,F**). Moreover, the C and O contents were also increased, which suggested the formation of an oxide and/or hydroxide layer and metal organic complex formed on the matrix surface. However, the crack distribution was increased on the VTACC surface and the V content decreased when the treatment time was increased further to 20 min. This effect was mainly due to internal stress from shrinkage during the drying stage and was also uniformly distributed on the substrate surface.

3.2 Electrochemical Measurement

The potentiodynamic measurements were applied to investigate the corrosion behavior of substrate and VTACCs obtained at different treatment times immersed in 3.5-wt% NaCl solution. Five typical polarization curves of coatings tested in 3.5-wt% NaCl solution showed that the cathodic and anodic reactions of AA6063 were both inhibited gradually with increased treatment time from 5 to 15 min (**Figure 2A**), which was mainly due to VTACC formation and covered the active area on the alloy and impeded electrolyte spread to the substrate (**Figures 1A–C**). However, when the treatment time was further prolonged to 20 min, the inhibition effect was weakened, due to the crack distribution generated on the VTACC surface (**Figure 1D**). The polarization resistance (R_p), corrosion potential (E_{corr}), and corrosion current density (I_{corr}) were obtained through Tafel

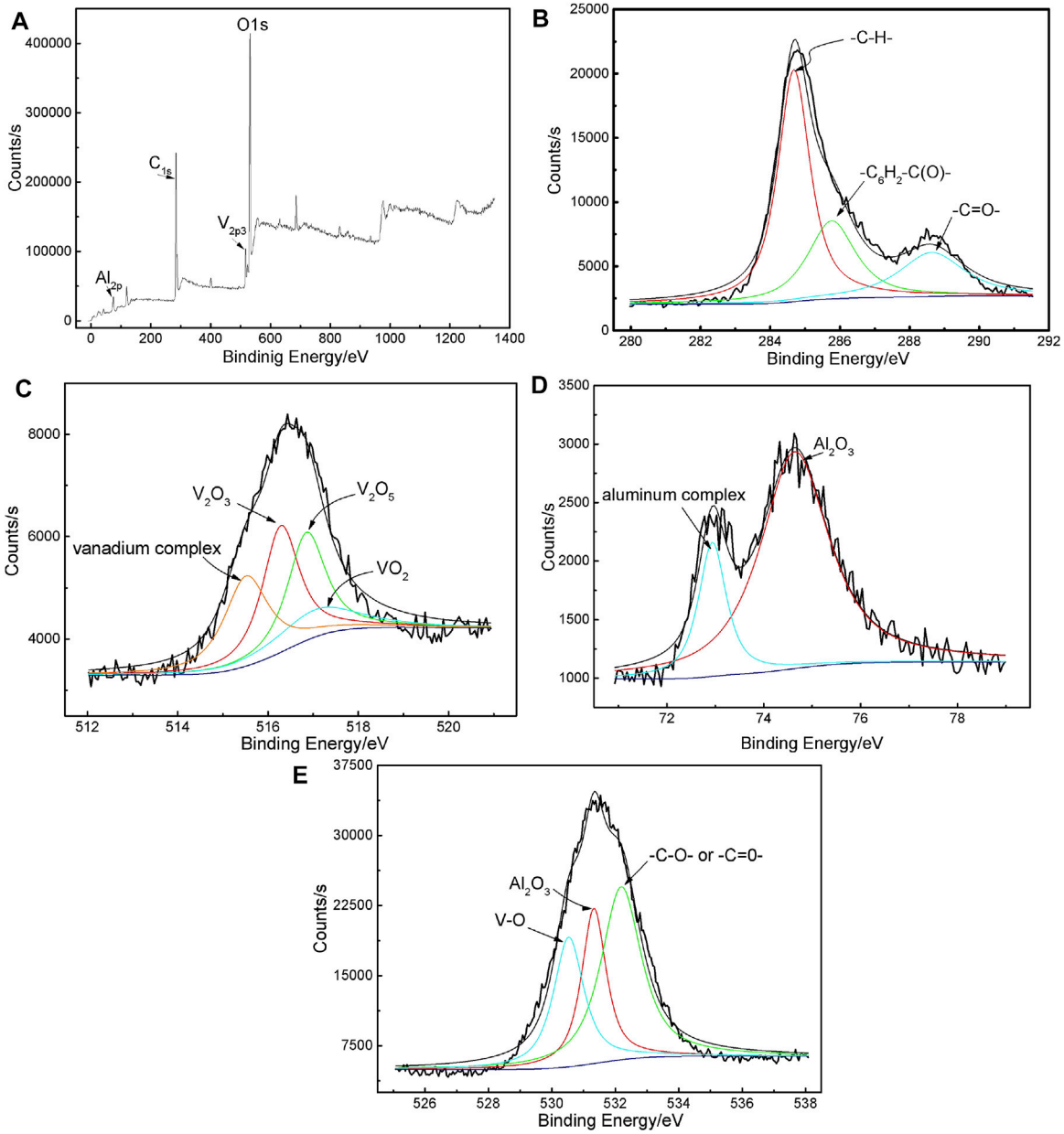

FIGURE 3 | XPS spectrum of VATCC on AA6063 **(A)** and high resolution deconvoluted XPS spectra of C-1*s*, V-2*p*, Al-2*p*, and O-1*s* [**(B–E)**, respectively].

extrapolation. The R_p was increased from 1.4×10^5 to $1.9 \times 10^5\ \Omega\ cm^2$. The E_{corr} was shifted in the positive direction by 302 mV, from −923 to −621 mV/SCE (**Figure 2B**). The I_{corr} was remarkably decreased from 2.94×10^{-7} to 7.2×10^{-8} A/cm^2 with increased from 0 to 15 min. However, the corrosion resistance of VTACC obtained at 20 min was inferior to that obtained at 15 min. Thus, the VATCC obtained at 15 min had better corrosion resistance (**Figures 2A,B**).

The corrosion behavior of VTACC obtained from different treatment times was detected by EIS measurement in 3.5-wt% NaCl solution. The loop diameter in Nyquist plots is related to the corrosion rate, and the larger diameter indicates better corrosion resistance (Shi et al., 2020). The semicircle diameter of VTACC clearly increased when the treatment time was 15 min, while it showed a slight decrease in semicircle diameter with 20 min treatment (**Figure 2C**). This semicircle diameter increase was ascribed to the inhibition effect of VTACC on the matrix and the decrease to the cracks on the VTACC surface reducing its barrier performance (**Figure 1**). The semicircle diameter of VTACC obtained from 10 min was close to that of VTACC from 15 min (**Figure 2C**). Thus, to find out the optimal formation time, EIS tests of VTACC from different treatment times for 11, 12, 13, and 14 min were performed in 3.5-wt% NaCl solution (**Figure 2D**). The semicircle diameter of VTACC obtained at

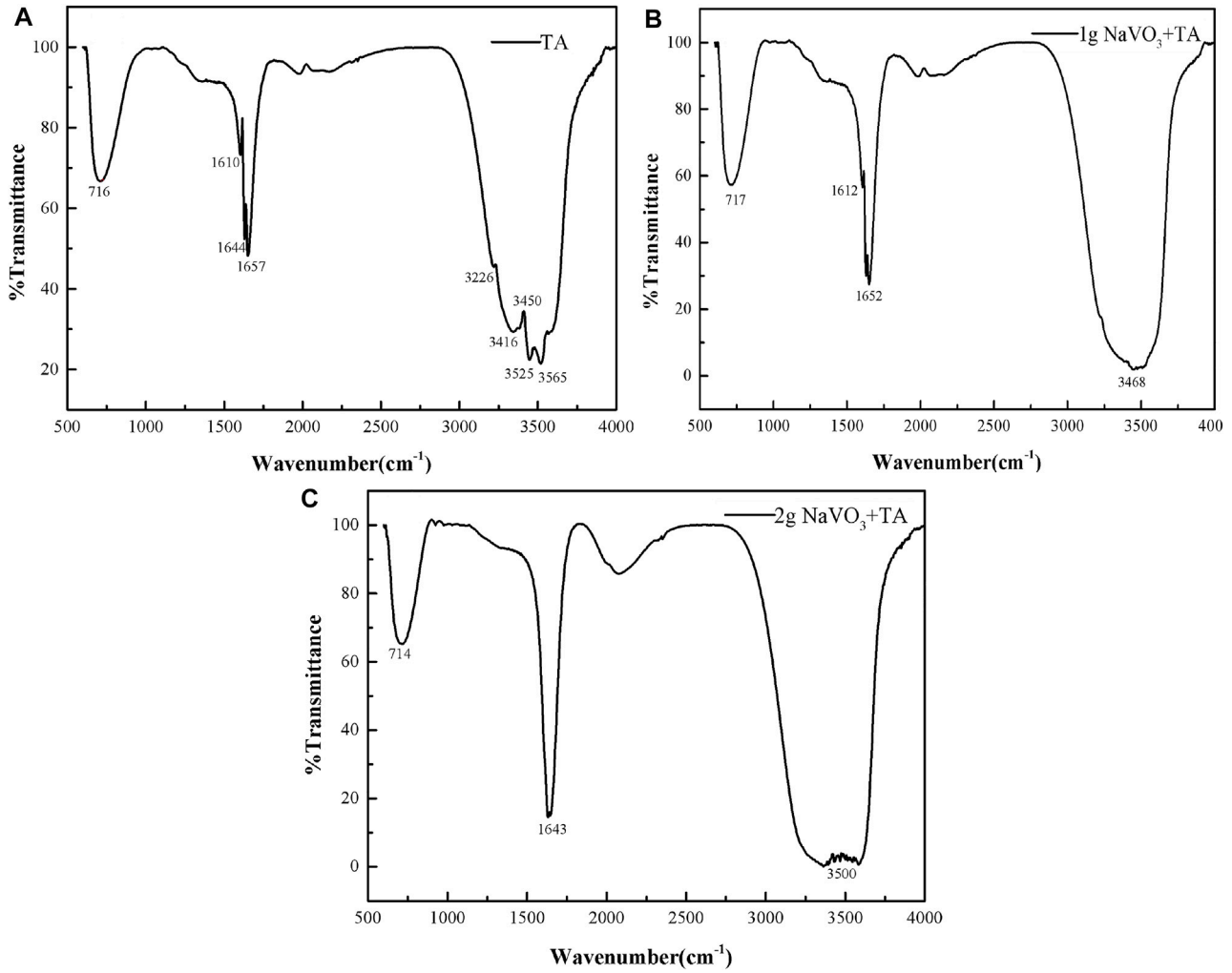

FIGURE 4 | Structural changes of VTA-based conversion solution during the aging process were investigated using FT-IR spectra from TA **(A)** and VTA solutions with different concentrations of sodium metavanadate **(B and C)**.

12 min was significantly greater than those of other VTACC times.

3.3 XPS Analysis

The chemical states of the elements in VTACC obtained from 12 min were determined by XPS analyses. The whole XPS spectrum showed that VTACC was mainly composed of C, O, Al, and V (**Figure 3A**), which was in accordance with the EDS results (**Figure 1**). High-resolution XPS spectra of C-1*s*, V-2*p*, Al-2*p*, and O-1*s* are presented in **Figures 3B–E**, respectively. The C-1*s* spectrum was decomposed to three peaks located at 284.4, 285.47, and 288.9 eV, corresponding to -C-H- in the organic polymer, -C_6H_4-C(O)- groups from the reaction product of TA, and C=O produced from TA (Chen et al., 2009), respectively. The photoelectron peak of V-2*p* was derived from four different oxidation states, with four peaks at 515.6, 515.9, 517.2, and 517.3 eV, assigned to V-complex, V_2O_3, V_2O_5, and VO_2 (Silversmit et al., 2004; Wu et al., 2004; Zou et al., 2011), respectively. The Al region in the XPS spectrum of Al–2*p* was composed of two peaks at 72.9 and 74.3 eV, which were attributed Al-complexation compounds and Al_2O_3 (Yi et al., 2012; Zuo et al., 2015; Zhu et al., 2016; Zhu et al., 2017), respectively. Three components with binding energies at 530.3, 531.5, and 532.5 eV were curve-fitted from the O-1*s* spectrum. The first peak at 530.3 eV was caused by V-O binding, the second ascribed to Al_2O_3, and the last at 532.5 eV is due to -C-O- or -C=O- (Yi et al., 2012; Zuo et al., 2015; Zhu et al., 2016; Zhu et al., 2017). According to these XPS analyses, the VTACC is mainly composed of metal oxides (Al_2O_3, V_2O_3, VO_2, and V_2O_5) and metal organic complexes (Al and V-complexes).

3.4 FT-IR Analysis

Structural changes of VTA-based conversion solution during the aging process were investigated using FT-IR spectra from TA (**Figure 4A**) and VTA solutions with different concentrations of sodium metavanadate (**Figures 4B,C**). There were three characteristic bands for TA solution, including hydroxide radical (OH^-) centered at 3,525 cm^{-1}, which indicated that there was a large

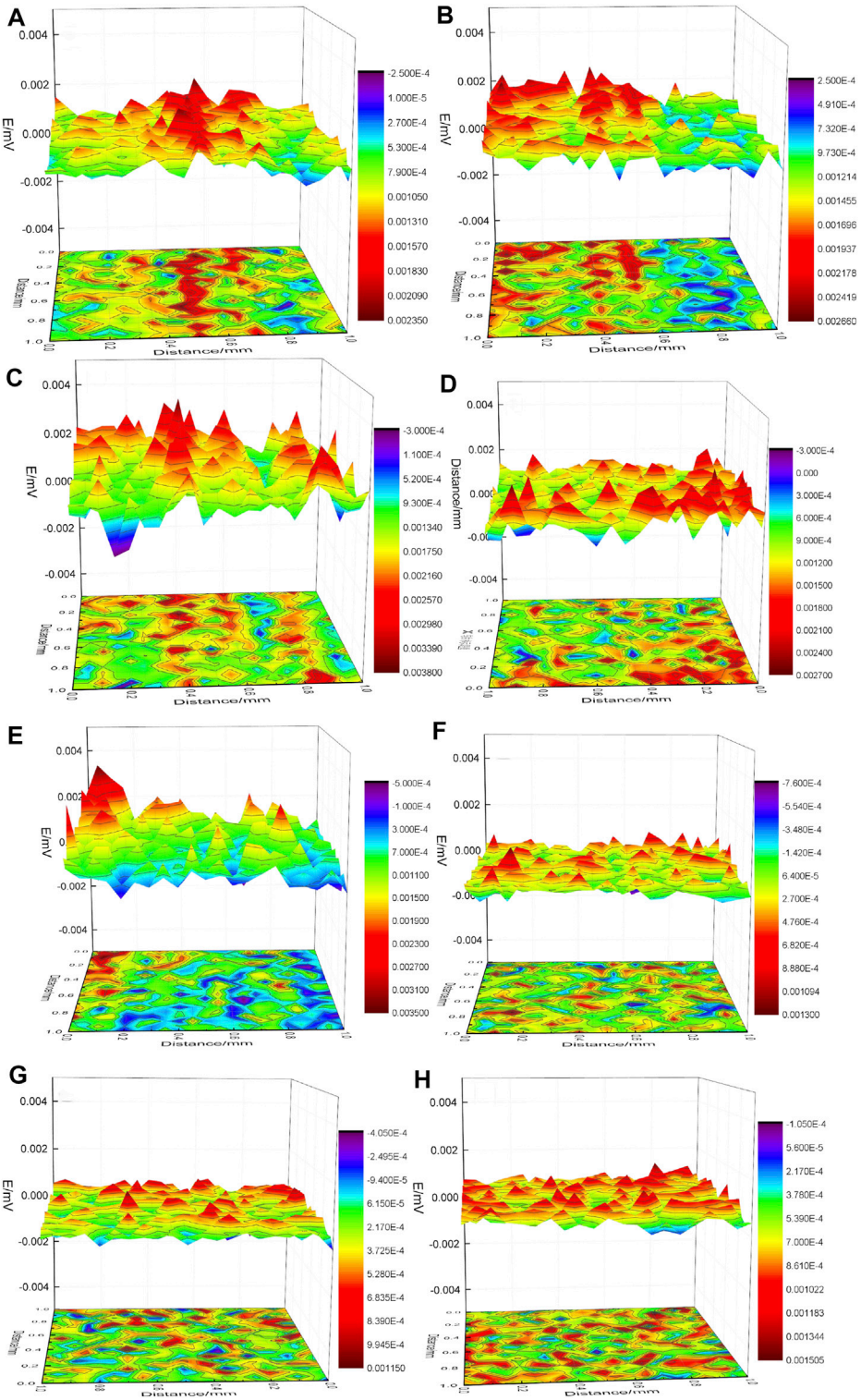

FIGURE 5 | SVET images of VTACCs with artificial scratches immersed in 3.5-wt% NaCl solution for different immersion times 0, 2, 4, 8, 12, 24, 32, and 48 h [**(A–H)**, respectively].

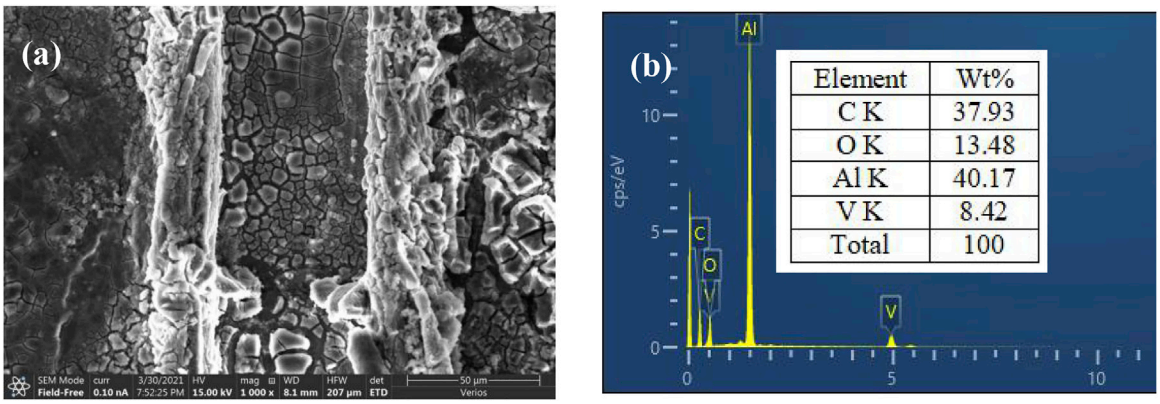

FIGURE 6 | SEM image **(A)** and EDS analysis **(B)** of artificial scratches on a VTACC surface after immersion in 3.5-wt% NaCl solution for 48 h.

number of strong polar phenol hydroxyls in this solution. The vibrations of the benzene ring skeleton were centered at 1,610, 1,644, and 1,657 cm^{-1}. The characteristic peak at 716 cm^{-1} corresponded to the out-of-plane bending vibrations of C-H on the benzene ring (Chen et al., 2009; Chen et al., 2008). The strength and location of three characteristics peaks changed significantly with the addition of 1 g $NaVO_3$ to 2 g/L tanic acid. When the added $NaVO_3$ was increased to 2 g, the width of the peak at 3,500 cm^{-1} became wider and the characteristic peaks at 1,610, 1,644, and 1,657 cm^{-1} disappeared, which was mainly because the functional groups in TA were oxidized by pentavalent vanadium (V^{5+}), which is a highly oxidizing species. The results indicated that TA was complexed with V in VTA-based conversion solution, resulting in the transformation of phenolic hydroxyl groups, which was consistent with XPS analysis (**Figure 3**). The complex reaction between tannic acid and vanadate ion had been reported in our previous work shown in Ref (Zhu et al., 2017), which included the tannic acid hydrolysizes and complexation reaction between gallic and VO^{2-}.

Based on the results of EDS, XPS, and FT-IR measurements, the mechanism of VTACC formation was concluded to involve the deposition of metal oxides and metal organic complexes.

The formation of VTACC was an electrochemically driven process (Andreatta et al., 2007), with many microbatteries produced on the matrix surface when the sample was immersed in conversion solution. The dissolution of Al was generated in micro-anodic sites and oxygen dissolution and hydrogen evolution produced in micro-cathodic sites. Meantime, OH^- produced in the above reaction led to increased local pH and thus triggered formation of V oxides and/or hydroxides. Simultaneously, V-organic complexes formed through TA complexation with metal ions, during solution aging and conversion treatment process, were adsorbed on the matrix surface. The above processes alternated to form a VTACC coating on the alloy surfaces.

3.5 SVET Test

SVET measurements were applied to monitor *in situ* the evolution of the self-healing ability in defective VTACC from 15 min treatment. A selected sequence of SVET images from different immersion times of artificial scratches on VTACC in 3.5-wt% NaCl solution for 0, 2, 4, 8, 12, 24, 32, and 48 h are shown in **Figure 5**. The corrosion activity was surveyed from the start of exposure in 3.5-wt% NaCl solution (**Figure 5A**). The voltage at the SVET tip increased along with the scratch as a function of solution immersion time, which was an indication of a high Al concentration in the zone, as a consequence of micro-anode processes in the coating defect (**Figures 5B,C**) (Andreatta et al., 2007; González-García et al., 2011). This process was observed as a progressive decrease in voltages, presented in selected cross-sections (**Figures 5D–F**), which was indicative of a low concentration of oxygen in the zone, as a consequence of micro-cathodic processes at these locations. The voltage of the partly scanned areas increased when immersion times more than 24 h, which was attributed to the observed pitting corrosion behavior (**Figures 5G,H**).

SEM images (**Figure 6A**) and EDS analysis (**Figure 6B**) of artificial scratches on VTACC surfaces after immersion in 3.5-wt% NaCl solution for 48 h showed that the new coating formed in a scratch mainly consisted of C, O, V, and Al and the contents of C and O more than that observed in **Figure 1F**, which implied the likely deposition of Al and V oxides and/or hydroxides in the scratch. The result indicated that V ion migration from the VTACC to the scratch area occurred during the immersion process and thus formed a new coating rich in V oxide.

5 CONCLUSION

A new VTACC was prepared on 6063 aluminum alloy surfaces and the optimal treatment time for the coating was found to be 12 min, according to the results of corrosion resistance measurements. On the basis of analytical results from SEM, EDS, and XPS, VTACC mainly consisted of Al_2O_3, V_2O_3, V_2O_5, and metal organic complexes. The results of SEM, EDS,

and SVET examining VTACC scratches indicated VTACC's self-healing performance resulted from the gradual disappearance of an artificial scratch on a VTACC surface with ongoing immersion time in 3.5-wt% NaCl solution. This was mainly because of the formation of a new coating rich in V oxides and/or hydroxides over the scratch area.

DATA AVAILABILITY STATEMENT

The original contributions presented in the study are included in the article/Supplementary Material. Further inquiries can be directed to the corresponding author.

AUTHOR CONTRIBUTIONS

All authors listed have made a substantial, direct, and intellectual contribution to the work and approved it for publication.

FUNDING

This work is financially supported by the Guangdong Basic and Applied Basic Research Foundation (Grant Nos. 2019A1515110466 and 2019A1515110913), the Dongguan Science and Technology of Social Development Program (Nos. 2020507140169 and 2020507140151), the Dongguan University of Technology (Nos. GC300502-45 and 300501-087), the Youth Innovative Talents Project of Guangdong University (No. 2021KQNCX099), and the Innovative Team Project of Guangdong University (No. 2021KCXTD022). The characterization results were supported by Beijing Zhongkebaice Technology Service Co., Ltd.

ACKNOWLEDGMENTS

We acknowledge critical and quantity of testing work supported by Beijing Zhongkebaice Technology Service Co., Ltd.

REFERENCES

Andreatta, F., Turco, A., de Graeve, I., Terryn, H., de Wit, J. H. W., and Fedrizzi, L. (2007). SKPFM and SEM Study of the Deposition Mechanism of Zr/Ti Based Pre-treatment on AA6016 Aluminum alloy. *Surf. Coat. Tech.* 201 (18), 7668–7685. doi:10.1016/j.surfcoat.2007.02.039

Aziz, I., Zhang, Q., and Du, J. (2011). Cerium-based thermal Conversion Treatments on Silicon Carbide Reinforced 2009 Aluminum alloy Composites. *Mater. Corrosion* 62 (3), 258–263. doi:10.1002/maco.200905485

Bertram, F., Zhang, F., Evertsson, J., Carlà, F., Pan, J., Messing, M. E., et al. (2014). *In Situ* anodization of Aluminum Surfaces Studied by X-ray Reflectivity and Electrochemical Impedance Spectroscopy. *J. Appl. Phys.* 116 (3), 034902–35105. doi:10.1063/1.4890318

Campestrini, P., Goeminne, G., Terryn, H., Vereecken, J., and de Wit, J. H. W. (2004). Chromate Conversion Coating on Aluminum Alloys. *J. Electrochem. Soc.* 151 (2), B59–B70. doi:10.1149/1.1637355

Campestrini, P., Terryn, H., Vereecken, J., and de Wit, J. H. W. (2004). Chromate Conversion Coating on Aluminum Alloys III. corrosion protection[J]. *J. Electrochem. Soc.* 151, B370–B377.

Campestrini, P., Terryn, H., Vereecken, J., and Wit, J. (2016). *Chromate Conversion Coating on Aluminum Alloys III. Corrosion Protection*. Doctoral dissertation, CN. CN101316816 B.

Chen, X., Li, G., Lian, J., and Jiang, Q. (2008). An Organic Chromium-free Conversion Coating on AZ91d Magnesium alloy. *Appl. Surf. Sci.* 255 (5p1), 2322–2328. doi:10.1016/j.apsusc.2008.07.092

Chen, X., Li, G., Lian, J., and Jiang, Q. (2009). Study of the Formation and Growth of Tannic Acid Based Conversion Coating on AZ91d Magnesium alloy. *Surf. Coat. Tech.* 204 (5), 736–747. doi:10.1016/j.surfcoat.2009.09.022

Chen, X., and Xu, S. (2021). Growth Process of Molybdate Conversion Coating on the Surface of Aluminum Foil and its Adhesive Mechanism. *Surf Interf. Anal* 53, 1048–1058. doi:10.1002/sia.7006

Chen, Y. F., Chen, C. M., Jie, Y. F., Meng, L., and Sheng, J. H. (2011). Temperature's Effection to Electroplating Ni-SiC Plating on Aluminum Alloy. *Amr* 189-193, 351–354. doi:10.4028/www.scientific.net/AMR.189-193.351

Cui, L.-Y., Liu, H.-P., Xue, K., Zhang, W.-L., Zeng, R.-C., Li, S.-Q., et al. (2018). *In Vitro* corrosion and Antibacterial Performance of Micro-arc Oxidation Coating on AZ31 Magnesium alloy: Effects of Tannic Acid. *J. Electrochem. Soc.* 165 (11), C821–C829. doi:10.1149/2.0941811jes

Dursun, T., and Soutis, C. (2014). Recent Developments in Advanced Aircraft Aluminium Alloys. *Mater. Des. (1980-2015)* 56, 862–871. doi:10.1016/j.matdes.2013.12.002

Gerengi, H., Slepski, P., Ozgan, E., and Kurtay, M. (2015). Investigation of Corrosion Behavior of 6060 and 6082 Aluminum Alloys under Simulated Acid Rain Conditions. *Mater. Corrosion* 66 (3), 233–240. doi:10.1002/maco.201307287

González-García, Y., Mol, J. M. C., Muselle, T., De Graeve, I., Van Assche, G., Scheltjens, G., et al. (2011). SECM Study of Defect Repair in Self-Healing Polymer Coatings on Metals. *Electrochemistry Commun.* 13 (2), 169–173. doi:10.1016/j.elecom.2010.12.005

Guan, Y., Liu, J. G., and Yan, C. W. (2011). Novel Ti/Zr Based Non-chromium Chemical Conversion Coating for the Corrosion protection of Electrogalvanized Steel. *Int. J. Electrochem. Sci.* 6 (10), 173. doi:10.1002/fuce.201000173

Hamdy, A. S., Doench, I., and Möhwald, H. (2011). Intelligent Self-Healing Corrosion Resistant Vanadia Coating for AA2024. *Thin Solid Films* 520 (5), 1668–1678. doi:10.1016/j.tsf.2011.05.080

Huang, Y., Mu, S., Guan, Q., and Du, J. (2019). Corrosion Resistance and Formation Analysis of a Molybdate Conversion Coating Prepared by Alkaline Treatment on Aluminum alloy 6063. *J. Electrochem. Soc.* 166 (8), C224–C230. doi:10.1149/2.1111908jes

Koroleva, E. V., Thompson, G. E., Hollrigl, G., and Bloeck, M. (1999). Surface Morphological Changes of Aluminium Alloys in Alkaline Solution:. *Corrosion Sci.* 41 (8), 1475–1495. doi:10.1016/s0010-938x(98)00188-7

Lay, P. A., and Levina, A. (1998). Activation of Molecular Oxygen during the Reactions of chromium(VI/V/IV) with Biological Reductants: Implications for Chromium-Induced Genotoxicities1. *J. Am. Chem. Soc.* 120 (27), 6704–6714. doi:10.1021/ja974240z

Li, K., Liu, J., Lei, T., and Xiao, T. (2015). Optimization of Process Factors for Self-Healing Vanadium-Based Conversion Coating on AZ31 Magnesium alloy. *Appl. Surf. Sci.* 353, 811–819. doi:10.1016/j.apsusc.2015.07.052

Li, X.-J., Zhang, M., Wen, S., Mao, X., Huo, W.-G., Guo, Y.-Y., et al. (2020). Microstructure and Wear Resistance of Micro-arc Oxidation Ceramic Coatings Prepared on 2A50 Aluminum Alloys. *Surf. Coat. Tech.* 394, 125853. doi:10.1016/j.surfcoat.2020.125853

Lunder, O., Simensen, C., Yu, Y., and Nisancioglu, K. (2004). Nisancioglu, Formation and Characterisation of Ti-Zr Based Conversion Layers on AA6060 Aluminium. *Surf. Coat. Tech.* 184 (2-3), 278–290. doi:10.1016/j.surfcoat.2003.11.003

Niu, L., Chang, S.-H., Tong, X., Li, G., and Shi, Z. (2014). Analysis of Characteristics of Vanadate Conversion Coating on the Surface of Magnesium alloy. *J. Alloys Compd.* 617, 214–218. doi:10.1016/j.jallcom.2014.08.044

Nordberg, G. F., Fowler, B. A., Nordberg, M., and Friberg, L. T. (2007). *Handbook on the Toxicology of Metals*, 79–100. doi:10.1016/B978-0-12-369413-3.X5052-6

Quievryn, G., Peterson, E., Messer, J., and Zhitkovich, A. (2003). Genotoxicity and Mutagenicity of Chromium(VI)/ascorbate-generated Dna Adducts in Human and Bacterial Cells. *Biochemistry* 42 (4), 1062–1070. doi:10.1021/bi0271547

Sheng, M., Wang, C., Zhong, Q., Wei, Y., and Wang, Y. (2010). Ultrasonic Irradiation and its Application for Improving the Corrosion Resistance of Phosphate Coatings on Aluminum Alloys. *Ultrason. Sonochem.* 17 (1), 21–25. doi:10.1016/j.ultsonch.2009.07.006

Shi, X., Wang, Y., Li, H., Zhang, S., Zhao, R., Li, G., et al. (2020). Corrosion Resistance and Biocompatibility of Calcium-Containing Coatings Developed in Near-Neutral Solutions Containing Phytic Acid and Phosphoric Acid on AZ31B alloy. *J. Alloys Compd.* 823, 153721. doi:10.1016/j.jallcom.2020.153721

Shida, A., Sugimura, H., Futsuhara, M., and Takai, O. (2003). Zirconium-phosphate Films Self-Assembled on Aluminum Substrate toward Corrosion protection. *Surf. Coat. Tech.* 169-170, 686–690. doi:10.1016/s0257-8972(03)00139-7

Silversmit, G., Depla, D., Poelman, H., Marin, G. B., and De Gryse, R. (2004). Determination of the V2p XPS Binding Energies for Different Vanadium Oxidation States (V5+ to V0+). *J. Electron Spectrosc. Relat. Phenomena* 135 (2-3), 167–175. doi:10.1016/j.elspec.2004.03.004

Twite, R. L., and Bierwagen, G. P. (1998). Review of Alternatives to Chromate for Corrosion protection of Aluminum Aerospace Alloys. *Prog. Org. Coat.* 33 (2), 91–100. doi:10.1016/S0300-9440(98)00015-0

Vega, J. M., Granizo, N., de la Fuente, D., Simancas, J., and Morcillo, M. (2011). Corrosion Inhibition of Aluminum by Coatings Formulated with Al-Zn-Vanadate Hydrotalcite. *Prog. Org. Coat.* 70 (4), 213–219. doi:10.1016/j.porgcoat.2010.08.014

Wu, Q.-H., Thissen, A., Jaegermann, W., and Liu, M. (2004). Photoelectron Spectroscopy Study of Oxygen Vacancy on Vanadium Oxides Surface. *Appl. Surf. Sci.* 236 (1-4), 473–478. doi:10.1016/j.apsusc.2004.05.112

Yang, K. H., Ger, M. D., Hwu, W. H., Sung, Y., and Liu, Y. C. (2015). Study of Vanadium-Based Chemical Conversion Coating on the Corrosion Resistance of Magnesium alloy. *Mater. Chem. Phys.* 101 (2-3), 480–485. doi:10.1016/j.matchemphys.2006.08.007

Yi, A. H., Li, W. F., Du, J., and Mu, S. L. (2012). Preparation and Properties of Chrome-free Colored Na3AlF6 Conversion Coating on Aluminum Alloy. *Amr* 490-495, 3527–3530. doi:10.4028/www.scientific.net/amr.490-495.3527

Zhang, S. F., Zhang, R. F., Li, W. K., Li, M. S., and Yang, G. L. (2012). Effects of Tannic Acid on Properties of Anodic Coatings Obtained by Micro Arc Oxidation on AZ91 Magnesium alloy. *Surf. Coat. Tech.* 207, 170–176. doi:10.1016/j.surfcoat.2012.06.056

Zhitkovich, A., Shrager, S., Messer, J., Marinkovic, J., Brzakovic, B., Pokrajac, M., et al. (2000). Reductive Metabolism of Cr(VI) by Cysteine Leads to the Formation of Binary and Ternary Cr–DNA Adducts in the Absence of Oxidative DNA Damage. *Chem. Res. Toxicol.* 13 (11), 1114–1124. doi:10.1021/tx0001169

Zhu, W., Li, W., Mu, S., Fu, N., and Liao, Z. (2017). Comparative Study on Ti/Zr/V and Chromate Conversion Treated Aluminum Alloys: Anti-corrosion Performance and Epoxy Coating Adhesion Properties. *Appl. Surf. Sci.* 405, 157–168. doi:10.1016/j.apsusc.2017.02.046

Zhu, W., Li, W., Mu, S., Yang, Y., and Zuo, X. (2016). The Adhesion Performance of Epoxy Coating on Aa6063 Treated in Ti/Zr/V Based Solution. *Appl. Surf. Sci.* 384, 333–340. doi:10.1016/j.apsusc.2016.05.083

Zou, Z., Li, N., Li, D., Liu, H., and Mu, S. (2011). A Vanadium-Based Conversion Coating as Chromate Replacement for Electrogalvanized Steel Substrates. *J. Alloys Compd.* 509 (2), 503–507. doi:10.1016/j.jallcom.2010.09.080

Zuo, K., Wang, X., Liu, W., and Zhao, Y. (2014). Preparation and Characterization of Ce-Silane-ZrO2 Composite Coatings on 1060 Aluminum. *Trans. Nonferrous Met. Soc. China* 24 (5), 1474–1480. doi:10.1016/S1003-6326(14)63215-5

Zuo, X., Li, W., Mu, S., Du, J., Yang, Y., and Tang, P. (2015). Investigation of Composition and Structure for a Novel Ti-Zr Chemical Conversion Coating on 6063 Aluminum alloy. *Prog. Org. Coat.* 87, 61–68. doi:10.1016/j.porgcoat.2015.05.008

Conflict of Interest: The authors declare that the research was conducted in the absence of any commercial or financial relationships that could be construed as a potential conflict of interest.